IFSCC 2025 full paper (IFSCC2025-1722)

"The Anti-inflammatory and Antioxidant Effects of Cell-Free Culture Supernatant of Probiotic *Staphylococcus epidermidis* CCSM0287 through the MAPK/NF-κB Signaling Pathways in HaCat cell induced by UVB"

Li Shao [1], Chunying Yuan [2], Suzhen Yang [2], Gang Liu [1], Hong Jiang [1], Laiji Ma [1] and Yan Li [2,*]

[1] College of Perfume and Aroma Technology, Shanghai Institute of Technology, Shanghai, China
[2] Research@Innovation Center, Shandong Freda Biotech Co., Ltd, Jinan, Shandong

1. Introduction

Ultraviolet B (UVB) radiation, which spans the wavelength range of 280–315 nm, is a well-known environmental stressor that plays a crucial role in skin damage. Prolonged or excessive UVB exposure is a major contributor to various skin disorders, including sunburn, premature aging, and genotoxicity, all of which can lead to serious dermatological conditions [1]. Among its harmful effects, UVB radiation induces the accumulation of reactive oxygen species (ROS) in the skin, which are highly reactive molecules that can cause cellular damage. ROS are produced as a result of the direct interaction of UVB radiation with cellular components such as lipids, proteins, and DNA, leading to oxidative stress [2]. This oxidative stress not only damages cellular structures but also triggers signaling pathways that contribute to skin inflammation, aging, and carcinogenesis [3]. ROS activate the MAPK and NF-κB signaling pathways. The MAPK signaling pathway increases the expression of inflammatory mediators, such as COX-2 and iNOS, which regulate inflammation and apoptosis and play a crucial role in immune response [4]. The NF-κB signaling pathway is involved in cytokine signaling, including interleukins and interferons, and its activation has been linked to conditions such as atopic dermatitis. The role of commensal skin microorganisms, particularly *Staphylococcus epidermidis*, is of significant interest in current research. *S. epidermidis* is a common skin-resident bacterium that plays a key role in skin immune defense [5]. It also possesses anti-inflammatory properties, such as inhibiting excessive immune responses, modulating cytokine expression, producing anti-inflammatory peptides, and promoting skin barrier restoration [6,7]. However, few studies have investigated *S. epidermidis* in the recovery from photodamage. Therefore, we investigated the anti-inflammatory capacity of S. epidermidis cell-free supernatant (CFS) and its underlying mechanism in a HaCaT cell inflammation model induced by UVB irradiation.

2. Materials and Methods

2.1 Bacterial strain and cells lines

S. epidermidis CCSM0287 was isolated, purified, and identified from healthy facial skin and deposited in the China Center for Type Culture Collection under accession number CCTCC M2022779. The strain was cultured in Trypticase Soy Broth (TSB) or Soybean-Casein Digest Agar at 37°C with/without shaking (160 r/min.). *S. epidermidis* CCSM0287 was cultured in TSB for 10 hours at steady-state, followed by centrifugation and filtration through 0.45 μm and 0.22 μm filters to obtain the cell-free supernatant (SE 287-CFS). Immortalized human

keratinocyte cells (HaCaT) were purchased from iCell Bioscience Inc (icellbioscience, iCell-h066, China). The cells were cultured in DMEM containing 4.5 g/L D-glucose supplemented with 10% fetal bovine serum at 37°C in a humidified atmosphere with 5% carbon dioxide. The cells were used for further experiments until they reached 80-90% confluence in plates.

2.2 UVB irradiation

HaCaT cells were seeded in a 96-well plate and exposed to UVB irradiation (10,20,30, and 40 mJ/cm^2) for 100-400 seconds at an intensity of 100 μW/cm² using a 311 nm UV lamp [3]. The cells were analyzed for viability and qPCR to establish optimal UVB conditions.

2.3 Cell viability

Cell viability was assessed using the Cell Counting Kit-8 (Biosharp, BS350b, China) after treatment with UVB and varying concentrations of SE 287-CFS. Absorbance at 450 nm was measured.

2.4 qPCR assay of mRNA expression of inflammatory cytokines

HaCaT cells were seeded into a 96-well plate at a density of 5 × 10^5 cells per well and incubated for 16 h. Total RNA was extracted from treated HaCaT cells and reverse transcribed to cDNA. qPCR was performed using EnTurbo™ SYBR Green PCR SuperMix (ELK Biotechnology, EQ001, China) and the QuantStudio 6 Flex System PCR Instrument, with GAPDH as the internal control. The primer sequences obtained were as follows: Human-TNF-α: CTCTTCTCCTTCCTGATCGTGG (forward) and CTTGTCACTCGGGGTTCGAG (reverse); Human-IL-6: ACTGGCAGAAAACAACCTGAAC (forward) and TTGTACTCATCTGCACAGCTCTG (reverse); Human-GAPDH: CATCATCCCTGCCTCTACTGG (forward) and GTGGGTGTCGCTGTTGAAGTC (reverse).

2.5 Experiment design

Cells were treated with SE 287-CFS at concentrations of 0%, 10%, 20%, 40%, 60%, 80%, and 100% (v/v) for 24 h, and with NAC at concentrations of 10, 20, and 30 μmol/L for 3 h. Similarly, 35 μL of medium was reserved for UVB irradiation at a dose of 30 mJ/cm², which was used to determine the optimal SE 287-CFS and NAC concentrations. Cells were then treated with 40% (v/v) SE 287-CFS for 4, 8, 12, 16, 18, and 20 h. The optimal treatment time for SE 287-CFS was determined under the 30 mJ/cm² UVB irradiation condition. The optimal SE 287-CFS treatment concentration and time were obtained.

2.6 Detection of cytokine

The production and expression of proinflammatory and anti-inflammatory cytokines in SE 287-CFS-treated HaCaT cells exposed to UVB irradiation were measured using ELISA kits. Cells were stimulated with 40% SE 287-CFS for 18 h. The supernatant was collected to measure the content of TNF-α (ELK Biotechnology, ELK1190, China), IL-1β (ELK Biotechnology, ELK1270, China), IL-6 (ELK Biotechnology, ELK1156, China), IL-8 (ELK Biotechnology, ELK1159, China), COX-2 (ELK Biotechnology, ELK5230, China), iNOS (ELK Biotechnology, ELK2643, China), and IL-10 (ELK Biotechnology, ELK1142, China) using ELISA kits, following the standard instructions.

2.7 Measurement of intracellular ROS production

The effects of SE 287-CFS on intracellular ROS levels in UVB-induced HaCaT cells were measured using 2',7'-Dichlorodihydrofluorescein diacetate (DCFH-DA) (Beyotime, S0033, China) as a fluorescent probe, according to the manufacturer's instructions [8]. The cells were imaged using a fluorescence microscope (Nikon, Eclipse Ci-L, Japan) immediately after staining was completed.

2.8 Detection of MDA, nitric oxide, SOD, CAT, and GSH level

HaCaT cells (5 × 10^5 cells per well) were seeded in 6-well plates. After treatment with 30 mJ/cm² UVB, 40% SE 287-CFS or 20 μmol/L NAC, MDA (Nanjing Jiancheng, A003-1, China), NO (Nanjing Jiancheng, A013-2, China), SOD (Nanjing Jiancheng, A001-1, China), CAT (Nanjing Jiancheng, A007-1, China), and GSH (Nanjing Jiancheng, A006-2, China) levels were measured in UVB-treated HaCaT cells using respective assay kits to evaluate lipid peroxidation and antioxidant capacity.

2.9 Western blot analysis

HaCaT cells (5 × 10^5 cells per well) were seeded into 6-well plates. Cells were treated with 40% SE 287-CFS for 18 h, followed by UVB stimulation at 30 mJ/cm^2. To acquire protein for analysis, the cells was homogenized and sonicated on ice using RIPA lysis buffer (ASPEN, AS1004, China). Immunoblotting was performed according to the method described by Xie et al [9] with slight modifications. The gray value of the target zone was analyzed using the AlphaEaseFC software.

2.10 Statistical analysis

The results are presented as the mean ± standard deviation (SD) of independent experiments conducted in triplicate. Statistical analysis was performed using one-way ANOVA (GraphPad Prism 9.5) and Duncan's multiple comparisons (SPSS 27.0). In one-way ANOVA, differences between groups were assessed, with (∗) $P < 0.05$, (∗ ∗) $P < 0.01$, (∗ ∗ ∗) $P < 0.001$, and (∗ ∗ ∗ ∗) $P < 0.0001$ considered statistically significant. ns indicated no significant difference. In Duncan's multiple comparisons, different letters indicate statistically significant differences ($P < 0.05$). Graphs were created using GraphPad.

3. Results

3.1 Establishment of UVB-introduce inflammatory cell model and determination of optimal treatment conditions for SE 287-CFS

As shown in Figure 1 (A-C), cells were exposed to UVB at doses of 0, 10, 20, 30, and 40 mJ/cm2, and cell viability and gene expression of TNF-α and IL-6 were measured. UVB exposure induced inflammation and cell damage, with significant reductions in cell viability ($P < 0.0001$) and elevated IL-6 ($P < 0.01$) and TNF-α ($P < 0.001$) gene expression at 30 mJ/cm2, making 30 mJ/cm² the optimal dose for the UVB-induced inflammation model. Under 30 mJ/cm2 UVB-induced inflammation, SE 287-CFS restored cell viability, with the highest viability (81.73 ± 7.40%) at 40% SE 287-CFS ($P < 0.05$), selected as the optimal concentration (Figure 1 D). NAC treatment (20 μmol/L) effectively restored cellular damage induced by UVB, confirming its role as a positive control. Finally, cell viability peaked at 18 hours of SE 287-CFS treatment (99.18 ± 4.28%), establishing 18 hours as the optimal treatment time (Figure 1 F).

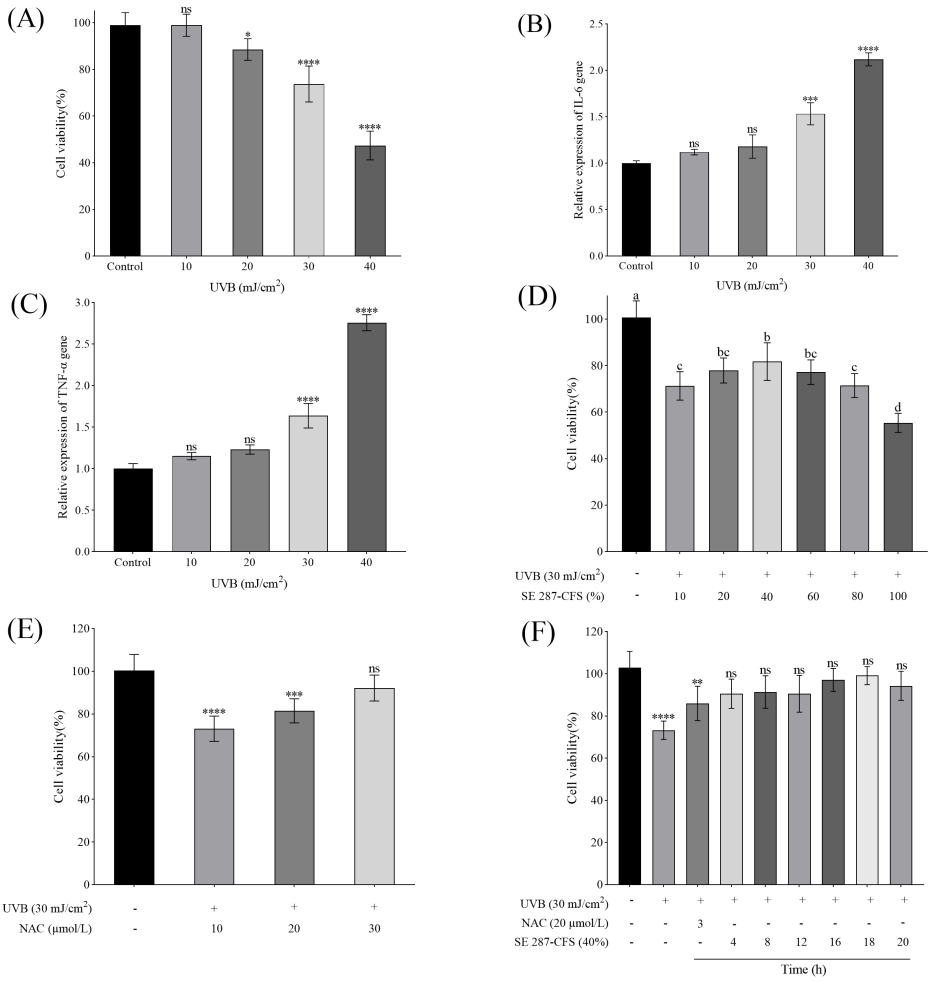

Figure 1. Establishment of a UVB-induced HaCaT cells inflammation model and the effect of SE 287-CFS on cell viability in the inflammation model. (A) Effect of different irradiation doses of UVB on cell viability. (B) Effect on UVB-induced IL-6 gene expression measured by qPCR. (C) Effect on UVB-induced TNF-α gene expression measured by qPCR. (D) Effect of different concentrations of SE 287-CFS on cell viability at 30 mJ/cm2 UVB irradiation dose. Duncan's multiple comparisons were used to test the significance of the differences, with $P < 0.05$ indicating a significant difference. (E) Effect of different concentrations of NAC on cell viability at 30 mJ/cm2 UVB irradiation dose. (F) Effect of different treatment times of 40% concentration of SE 287-CFS on cell viability at 30 mJ/cm2 UVB irradiation dose.

3.2 Effect of S. epidermidis CCSM0287 on UVB-induced NO production, the secretion of cytokines and ROS production

As shown in Figure 2, Compared with UVB group, pretreatment with 40% SE 287-CFS significantly reduced the expression of these cytokines, and fluorescence photos showed that the content of ROS decreased significantly ($P < 0.0001$), the content of NO decreased from (46.23 ± 5.86) μmol/L to (22.55 ± 3.67) μmol/L ($P < 0.001$), and the expression level of IL-10 decreased from (6.17 ± 1.63) to (18.93 ± 2.92) pg/mL. These results indicate that SE 287-CFS can alleviate UVB-induced inflammation.

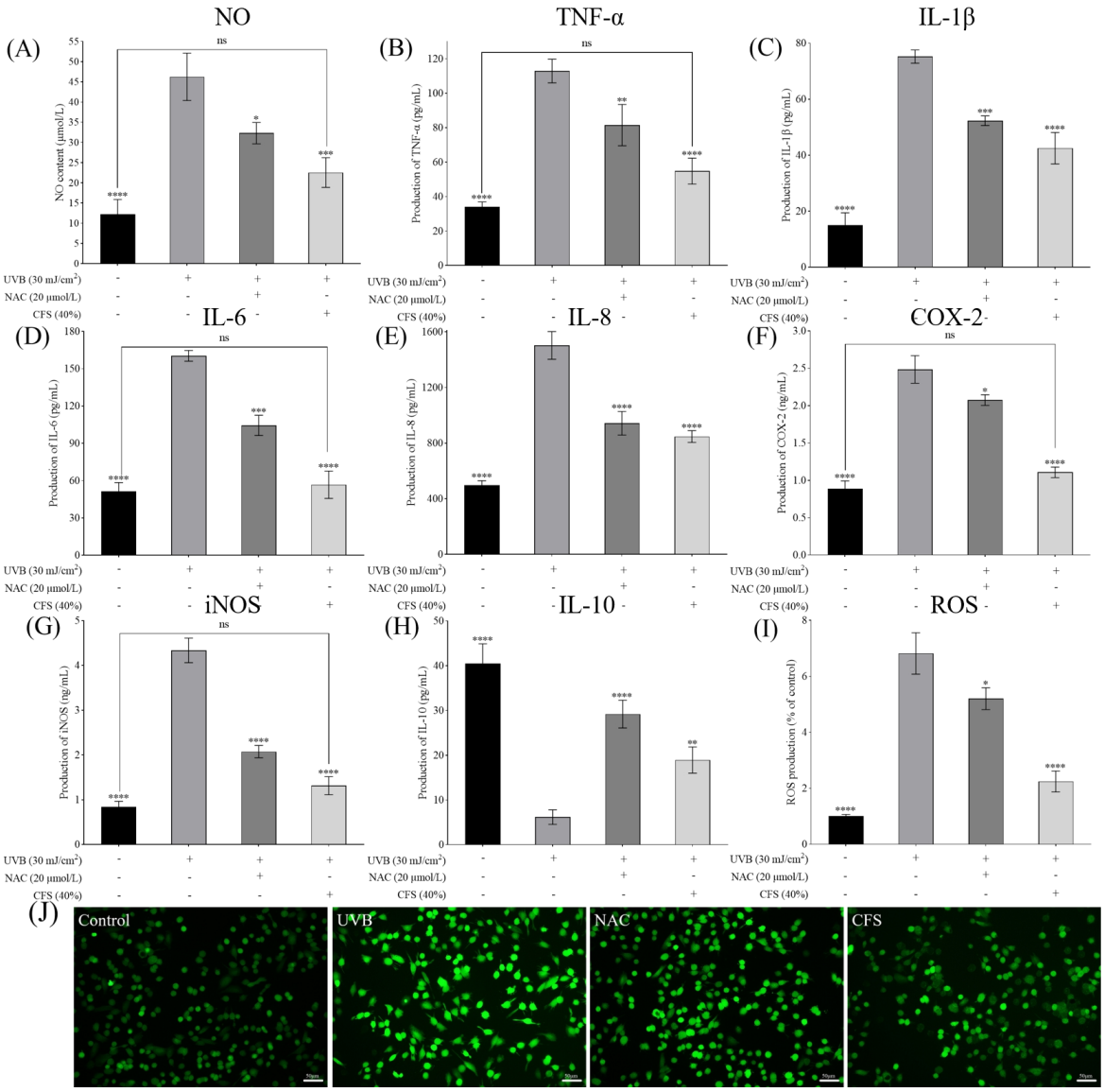

Figure 2. The effect of *S. epidermidis* CCSM0287 diminished UVB-induced proinflammatory response by modulating cytokines and mediators of inflammation. (A) NO content in HaCaT cells of different treatment groups. ELISA assay of (B) TNF-α, (C) IL-1β, (D) IL-6, (E) IL-8, (F) COX-2, (G) iNOS and (H) IL-10 in HaCaT cells of different treatment groups. (I) Comparison of ROS fluorescence intensity in HaCaT inflammatory cells of different treatment groups. (J) Fluorescence image of ROS content on 40% concentration of SE 287-CFS treated UVB-induced HaCaT cell model measured by DCFH-DA probe (Bars = 50 μm).

3.3 SE 287-CFS inhibits LPS-induced oxidative stress levels

UVB exposure significantly increased MDA levels and decreased SOD, CAT, and GSH activities in HaCaT cells. SE 287-CFS (40%) reduced MDA to (5.68 ± 0.35) nmol/mg protein ($P < 0.0001$) and significantly enhanced SOD, CAT, and GSH activity, demonstrating its antioxidative effect against UVB-induced oxidative stress (Figure 3).

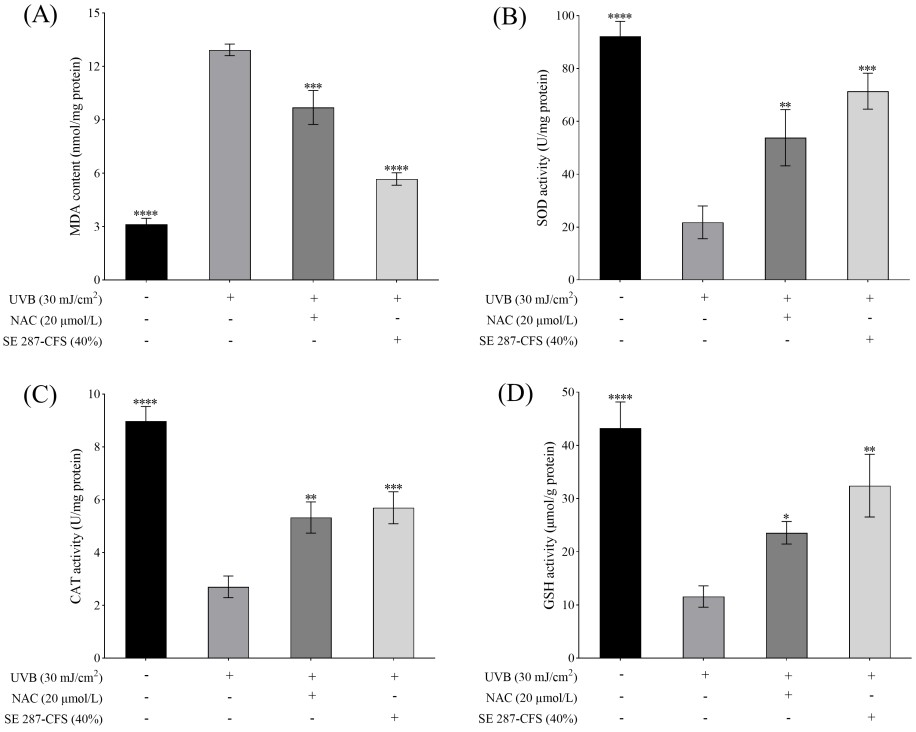

Figure 3. Changes of intracellular MDA and antioxidant enzymes after UVB irradiation by *S. epidermidis* CCSM0287. (A) MDA content of HaCaT cells in each group. (B) SOD activity, (C) CAT activity, and (D) GSH activity of HaCaT cells in each group.

3.4 SE 287-CFS inhibits UVB-induced inflammatory effects through MAPK and NF-κB pathways in HaCaT cells

As shown in Figure 4, protein blot analysis proved that UVB irradiation significantly activated the phosphorylation of JNK, p38 and ERK in MAPK signal pathway and p65, IκBα and IKKβ in NF-κB signal pathway. However, in UVB-induced cells, SE 287-CFS treatment significantly reduced the phosphorylation of the above proteins.

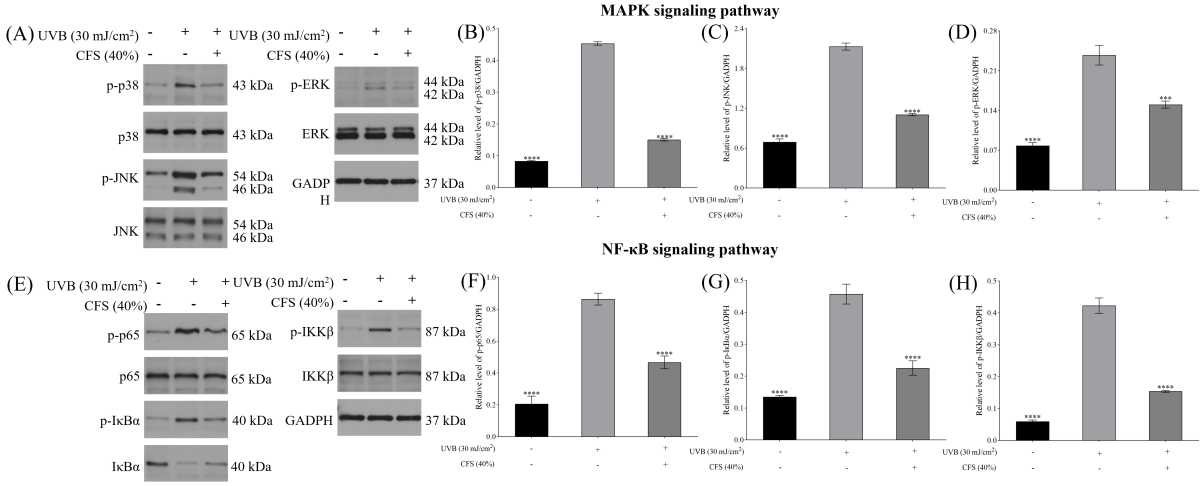

Figure 4. Effect of *S. epidermidis* CCSM0287 on the MAPK and NF-κB signaling pathway in UVB-irradiated HaCaT cells. (A) Western blotting analysis on production of MAPK and phosphorylated MAPK. ImageJ normalized quantitative analysis of the p-p38/GADPH (B), p-JNK/GADPH (C) and p-ERK/GADPH (D) ratios from immunoblots in (A). (E) Western blotting analysis on production of NF-κB and phosphorylated NF-κB. ImageJ normalized quantitative analysis of the p-p65/GADPH (F) p-IκBα/GADPH (G) and p-IKKβ/GADPH (H) ratios from immunoblots in (E).

4. Discussion

UVB irradiation is a well-established environmental stressor that triggers the production of reactive oxygen species (ROS), leading to oxidative stress, inflammation, and ultimately cellular apoptosis [10]. Our results align with previous studies that show UVB exposure significantly elevates the levels of ROS in skin cells, particularly in HaCaT cells, which are frequently used as a model for studying skin responses. The elevated ROS levels cause cellular damage by interacting with proteins, lipids, and DNA, resulting in oxidative stress. In response to this, inflammatory pathways are activated, contributing to the onset of various skin disorders. One of the key biomarkers of oxidative stress is malondialdehyde (MDA), a product of lipid peroxidation, which we observed to be significantly increased in UVB-exposed HaCaT cells. However, treatment with *S. epidermidis* CCSM0287 notably reduced both ROS accumulation and MDA levels, suggesting that this strain plays a critical role in mitigating oxidative damage. Furthermore, *S. epidermidis* CCSM0287 restored the activity of important antioxidant enzymes, including superoxide dismutase (SOD), catalase (CAT), and glutathione (GSH), which are typically depleted during UVB-induced oxidative stress.

In addition to oxidative stress, UVB exposure stimulates the production of nitric oxide (NO), which is closely linked to inflammation and the pathogenesis of several inflammatory skin conditions, such as psoriasis and atopic dermatitis [11]. UVB-induced NO production is associated with an increase in the expression of pro-inflammatory cytokines, such as IL-1β and TNF-α, both of which are critical mediators in the inflammatory cascade. Our findings demonstrated that *S. epidermidis* CCSM0287 effectively reduced the expression of these pro-inflammatory cytokines, further highlighting its anti-inflammatory potential. More importantly, this strain promoted the production of IL-10, a key anti-inflammatory cytokine that plays an essential role in resolving inflammation and facilitating tissue repair.

Additionally, *S. epidermidis* CCSM0287 was shown to inhibit the activation of two critical inflammatory signaling pathways, MAPK and NF-κB. UVB exposure activates MAPK signaling, leading to the phosphorylation of key members such as JNK, p38, and ERK, which regulate various cellular processes including inflammation and apoptosis [12]. Similarly, UVB-induced ROS triggers the NF-κB pathway, leading to the phosphorylation of p65, IκBα, and IKKβ, promoting the expression of inflammatory mediators. Our results indicate that *S. epidermidis* CCSM0287 significantly inhibited the phosphorylation of both MAPK and NF-κB components, suggesting that it prevents the downstream inflammatory responses induced by UVB irradiation. These findings underscore the potential of *S. epidermidis* CCSM0287 as a protective agent against UVB-induced skin damage, not only by modulating oxidative stress but also by regulating key inflammatory pathways.

5. Conclusion

This study provides strong evidence for the anti-inflammatory properties of *S. epidermidis* CCSM0287 CFS in alleviating UVB-induced skin inflammation. The results demonstrate that CFS significantly reduces oxidative stress markers, including ROS, MDA, and pro-inflammatory mediators such as TNF-α, IL-1β, IL-6, IL-8, COX-2, and iNOS. Additionally, CFS activates antioxidant defenses, including SOD, GSH, and CAT, and enhances the expression of the anti-inflammatory cytokine IL-10. The findings show that CFS exerts its anti-inflammatory effects by modulating key signaling pathways, specifically the MAPK and NF-κB pathways. CFS inhibits the phosphorylation of key components of these pathways, including p38, JNK, ERK, p65, IκBα, and IKKβ, which are critical to the inflammatory response. In conclusion, these findings indicate that CCSM0287 exhibits strong anti-inflammatory and antioxidant properties, effectively mitigating UVB-induced photodamage. This establishes a solid basis for utilizing skin probiotics in anti-photodamage research, mechanistic studies, and the development of bacterial-derived cosmetic ingredients for skin health.

6. Reference

[1] Choi S I, Han H S, Kim J M, et al. *Eisenia bicyclis* extract repairs UVB-induced skin photoaging in vitro and in vivo: photoprotective effects[J]. Marine Drugs, 2021, 19(12): 693.

[2] Yang J, Das B C, Aljitawi O, et al. Magmas inhibition in prostate cancer: A novel target for treatment-resistant disease[J]. Cancers, 2022, 14(11): 2732.
[3] Li Y, Ma Y, Yao Y, et al. Protective effect of isoquercitrin on UVB‐induced injury in HaCaT cells and mice skin through anti‐inflammatory, antioxidant, and regulation of MAPK and JAK2‐STAT3 pathways[J]. Photochemistry and Photobiology, 2024, 100(5): 1507-1518.
[4] Fang M, Zou T, Yang X, et al. Discovery of novel pterostilbene derivatives that might treat sepsis by attenuating oxidative stress and inflammation through modulation of MAPKs/NF-κB signaling pathways[J]. Antioxidants, 2021, 10(9): 1333.
[5] Lai Y, Di Nardo A, Nakatsuji T, et al. Commensal bacteria regulate Toll-like receptor 3–dependent inflammation after skin injury[J]. Nature medicine, 2009, 15(12): 1377-1382.
[6] Ochlich D, Rademacher F, Drerup K A, et al. The influence of the commensal skin bacterium Staphylococcus epidermidis on the epidermal barrier and inflammation: Implications for atopic dermatitis[J]. Experimental Dermatology, 2023, 32(4): 555-561.
[7] Harris-Tryon T A, Grice E A. Microbiota and maintenance of skin barrier function[J]. Science, 2022, 376(6596): 940-945.
[8] Zhang M, Qin H, Xiang L, et al. Camellia sinensis polysaccharide attenuates inflammatory responses via the ROS-mediated pathway by endocytosis[J]. International Journal of Biological Macromolecules, 2024, 267: 131674.
[9] Xie Z, Wang Y, Huang J, et al. Anti-inflammatory activity of polysaccharides from *Phellinus linteus* by regulating the NF-κB translocation in LPS-stimulated RAW264. 7 macrophages[J]. International journal of biological macromolecules, 2019, 129: 61-67.
[10] Mohamed H R H, Hemdan S H A, El-Sherif A A. Y2O3NPs induce selective cytotoxicity, genomic instability, oxidative stress and ROS mediated mitochondrial apoptosis in human epidermoid skin A-431 Cancer cells[J]. Scientific Reports, 2025, 15(1): 1543.
[11] Camillo L, Gironi L C, Zavattaro E, et al. Nicotinamide attenuates UV-induced stress damage in human primary keratinocytes from cancerization fields[J]. Journal of Investigative Dermatology, 2022, 142(5): 1466-1477. e1.
[12] An Y, Zhang H, Wang C, et al. Activation of ROS/MAPKs/NF-κB/NLRP3 and inhibition of efferocytosis in osteoclast-mediated diabetic osteoporosis[J]. The FASEB Journal, 2019, 33(11): 12515.